Optimal operation of large district heating networks through fast fluid-dynamic simulation

POSTPRINT: Guelpa E., Toro C., Sciacovelli A., Melli R., Sciubba, E., Verda, V. (2016). Optimal operation of large district heating networks through fast fluid-dynamic simulation. Energy 102: 586-595

Optimal operation of large district heating networks through fast fluid-dynamic simulation

Elisa Guelpa[a], Claudia Toro[b], Adriano Sciacovelli[c], Roberto Melli[d], Enrico Sciubba[e], and Vittorio Verda[f]

[a] *Politecnico di Torino Energy Department, Torino, Italy, elisa.guelpa@polito.it*
[b] *CNR Institute of Environmental Geology and Geoengineering IGAGc/o Dept of Mechanical and Aerospace Engineering University of Rome " Sapienza", Rome, Italy, claudia.toro@uniroma1.it*
[c] *School of Chemical Engineering – Birmingham Centre for Energy Storage (BCES) University of Birmingham, Edgbaston, Birmingham, UK, a.sciacovelli@bham.ac.uk*
[d] *University of Rome "Sapienza" Dept of Mechanical and Aerospace Engineering, Rome, Italy, roberto.melli@uniroma1.it*
[e] *University of Rome "Sapienza" Dept of Mechanical and Aerospace Engineering, Rome, Italy, enrico.sciubba@uniroma1.it*
[f] *Politecnico di Torino Energy Department, Torino, Italy, vittorio.verda@polito.it*

Abstract

Optimization of the operating conditions of district heating networks is usually performed limiting the analysis to the primary energy related with heat production. An additional aspect that should be considered is the role played by the pumping system. Pumping may contribute to about 10% of the total primary energy consumption, especially in large networks or when small temperature levels are applied. Furthermore, the increasing share of waste heat or renewable energy sources from distributed producers requires a flexible and efficient pumping system. A further aspect which pumping strategy should face is system operation when malfunctions in the plants, pumps or pipes occur.

Optimization of the pumping system requires the use of detailed simulation tools, which may need significant computational resources, especially in the case of large networks. A reduced model, based on Proper Orthogonal Decomposition combined with Radial basis functions (POD-RBF model) is proposed in this paper. This approach allows maintaining high level of accuracy despite reductions of more than 80% in the computational time. This make the approach effective tool for control strategy operations. An application to a large district heating network shows that reductions of about 20% in the pumping request and effective management of failures are possible.

Keywords:
Proper Orthogonal Decomposition, model reduction, district heating network, pumping cost, hydraulic model

1. Introduction

District heating (DH) is considered a very efficient option for providing heating and domestic hot water to buildings, particularly when they are located in densely populated areas [1]. The main advantage of DH systems consists in the possibility of utilizing the waste heat from industries or waste-to-energy plants or the heat generated by a number of efficient/low carbon thermal plants, such as cogeneration plants, and biomass [2], solar [3] and geothermal [4] systems.

An important aspect to achieve high efficiency in DH is the optimization of the operating conditions the system has to face in order to comply with the household thermal request. In the literature, various papers deal with the analysis of supply temperature during daily [5] and seasonal [6] operations or with the selection of the optimal supply and return temperatures [7]. In [8] a control approach is proposed in order to increase the temperature difference across the substations with a consequent increase of overall performances. In [9], the operating conditions of a district heating system are optimized acting both on the set-point temperature of the boilers and on the water flow of the pumps; the total fuel consumption is considered as the objective function to be minimized. In [10] and [11] the opportunities to modify the thermal request profile of some users are investigated to maximize the heat production from cogeneration or renewable plants.

An important aspect of optimal strategy analysis refers to pumping systems. Pumping systems are used to fulfill the desired heat flux to users facing the issues related to variations in friction losses. They include a set of pumps located along the network to provide consumers with hot water from the heat generation plants. The energy consumed for pumping operations is not negligible, in particular in large district heating networks, when distances involved are long. This aspect is further stressed in the case of low temperature district heating systems, typically operating with small temperature differences between supply and return networks and large mass flow rates [12]. Moreover, pumps work continuously during the heating season, even when heat demand is low.

For instance, the DH system of the city of Turin, which is considered in this work as a case study, requires up to about 6 MW of power transferred to the fluid, depending on the thermal load. This means that pumping represents about 2% of the primary energy consumption at peak request and increases to about 6-8% at night.

This aspect is also highlighted by various papers in literature, proposing the implementation of fluid dynamic models of the network for design purpose or the analysis of the effects of the control strategy on the energy consumption. A method for district heating network dimensioning, based on the probabilistic determination of the flow rate for hot water heating was carried out in [13]. Network costs, pumping energy consumption, and power of boilers were considered. In [14] a multi-objective optimization model is performed for the best network design considering both initial investment for pipes and pumping cost for water distribution. The best pipe diameters that reduce the total cost have been evaluated. A technical-economical optimization with the aim of minimizing both the pumping energy consumption and the thermal energy losses while maximizing the yearly annual revenue is performed in [15]. In [16] a fluid-dynamic model solved with the Hardy Cross method [17] is used in order to compare hydraulic performances of distributed variable speed pumps and conventional central circulating pump. Stevanovic et al. [18] solve the fluid-dynamic model with a loop method in order to show the potential for energy savings in pumping operations; the loop method is shown to be more effective with respect to the Hardy Cross method that is affected by problems related to convergence, computational cost and limited use [19]. In [20] a fluid-dynamic model of the network based on conservation was built and a genetic algorithm used in order to minimize the energy required by the system. Most works available in literature are focused on small district heating networks. When a large district heating network is considered, the computational cost to solve a physical based model becomes very high; this excludes the use of full physical models for fast multi-scenario and fast optimization applications.

In the present paper, the authors present two different model approaches for the simulation of large networks and the analysis of the optimal control strategy for the pumping system. The two models are built in order to find the set of pumping pressures that should be applied to the pumps located along the network so as to minimize the total electricity consumption for a given operating scenario. The first model is a fluid-dynamic model based on mass and momentum conservation equations which consider the network topology through a graph approach. The second method is a reduced model, which has been derived from the fluid-dynamic model. Model reduction is obtained through the combination of proper orthogonal decomposition (POD) and radial basis functions (RBF). POD is a reduction technique which is able to decrease the computational cost of full physical models without losing the most relevant information. POD is able to capture the main features of a complex problem using a smaller degree of information (eigenfunctions) than the full model.

This method has received much attention for the reduction of complex physical systems and it has been used in different fields of science and engineering, such as the analysis of turbulent fluid flows [21,22], unsteady thermal systems [23], image processing [24] and many other fields.

Both the full physical model and the POD-RBF model are used in order to find the optimal set of pumping pressures that minimize the mechanical power that should be applied to the working fluid (i.e. the efficiency of the pump and the efficiency in the overall energy supply chain from primary energy to electricity production have not been considered) to fulfill the thermal requests of the various users, once the heat production of each plant is fixed. In the following, this objective function has been indicated as pumping cost, which should be intended as a cost expressed in energy units. An analysis with different thermal loads was performed because of the peculiar characteristics of district heating networks to work for a large number of operating hours in off-design conditions. Therefore a careful analysis of optimal operating conditions, with different thermal requests, is necessary to achieve high levels of the annual efficiency. The heat flow supplied by each thermal plant is provided as an input of the model by setting the water mass flow rates exiting the various plants.

Results obtained with the two models are compared in terms of both minimum energy consumption and computational time for each thermal load. The POD-RBF model allows us to obtain optimal costs that differ from the cost provided by the full physical model of less than5%. The full physical model is extremely time-consuming especially if applied to large district heating networks. The POD-RBF method is much faster than the full physical model and allows us to perform multiple simulations and optimizations using small computational resources. The POD-RBF approach is shown to be very effective for the optimal management of complex district heating systems reducing computational cost by more than 90% with respect to the full physical model. This allows the optimization process for a much larger number of scenarios. Results of the optimization are then compared with the current pumping strategy used for the district heating system of the city of Turin; the comparison shows that a change in the policy of pumping operations can reduce the energy consumption for pumping by about 20%.

2. System description

The Turin district heating network is the largest network in Italy. It currently connects about 55000 buildings with an annual thermal request of about 2000 GWh. The maximum thermal power is about 1.2 GW. An expansion of the system, to reach about 72 million cubic meters of buildings is already planned [25].The water supply temperature is constant and its value is 120°C while the return temperature varies with mass flow rate in the network and thermal load; the mean value is 65 °C.

The complete network can be considered as composed of two parts: a transport network and a distribution network. The transport network, consists in large diameter pipes, usually larger than 200 mm, and connects the thermal plants to the thermal barycentres. Each barycentre is a subnetwork that reaches a group of buildings that are located in the same area. In the Turin network there are 182 barycentres. The ensemble of these sub-networks constitutes the distribution network. The transport network is a loop network, while the sub-networks are tree-shaped networks. Figure 1 depicts the transport pipeline network and, in detail, 3 barycentres with their corresponding tree-shaped networks.

The model developed in this work only considers the main transport network. The total length is about 515 km. Five thermal plants, which are highlighted in green in Figure1, provide heat to the network. The main characteristics of the plants are reported in Table 1. The most usual start-up strategy of the thermal plants is the following: the two cogeneration plants in Moncalieri are started-up first (when the thermal request is below 260 MW one plant is operating, while the second one is operating when the request is below 520 MW), then the cogeneration plant in Torino Nord is started up and then the storage units in Politecnico and in Torino Nord. Larger thermal requests are covered using the boilers in Politecnico, Torino Nord, Mirafiori Nord, BIT, Moncalieri. In the case some of the plants are not available or when specific constraints due to electricity production must be fulfilled, a different order can be selected.

Regarding pumping systems, the main pumping stations are located at the thermal plants and 9 booster pump groups are located along the network. The main pumping stations allow the desired hot mass flow rate to be pumped into the network, from the operating thermal plants to the users. Booster pumping stations are used in order to distribute the correct mass flow rate to each user, contrasting friction losses and hydraulic head. Booster pumping stations and direction of the pumped flow are indicated in Figure 1b. RP1 and RP2 include two groups of pumps, each pumping in a specific direction; RP5 includes three groups of pumps; RP3 and RP4 include only one group of pumps. The latter is not considered in the simulation because it is used in a

network configuration different to that examined in this work. The use of RP4 will be necessary when the network developments, which are already planned, are completed. A further utilization of this pump is possible in the case of malfunctions.

3. Models description

In order to minimize the pumping energy consumption, to provide the users with their thermal request, an optimization was performed. In the optimization, each scenario is defined by setting the total thermal load and the contribution of each plant to the thermal load, i.e. the heat production of each plant does not vary in the optimization procedure. Mass flow rates at the various plants are obtained dividing the heat production by the specific heat and the temperature difference between supply and return network.

There are various different settings of the pumping groups which allow combining the production of plants and the request of the users, each corresponding with a different total power consumption. The independent variables are the pressure differences in the pumping stations; therefore there are 8 independent variables, one for each pump located along the network. As previously discussed, only the booster pumping stations, not the pumps located in the plants, were considered. A maximum pressure of 17 bar has been set as a technical constraint.

The objective function is the energy consumption, also called the energy cost. It has been calculated as:

$$C = \sum_p \frac{G_p \Delta p_p}{\rho} + \sum_r \frac{G_r \Delta p_r}{\rho} \quad (1)$$

where subscript p indicates pumping systems located in the thermal plant, which are the dependent variables in the optimization problem, and subscript r indicates the booster pumping systems, which are the independent variables. The water density in the plants was evaluated as the average value between the supply and the return temperatures. This procedure should be repeated for different thermal loads in order to build an optimal control strategy.

Two approaches have been used to perform the optimization: a fluid dynamic approach and a POD approach. As regards the fluid dynamic approach, a genetic algorithm[26] was applied to the model described in the next section. The algorithm starts the search for the optimal values from multiple initial points. Consequently various cases (also called individuals in literature) must be created to run the optimization. This set of cases is usually named the population. The number of individuals in the population is kept constant during the

optimization process, but the values of the independent variables associated with each individual are modified at each iteration. Iterations are usually called generations in GA nomenclature. To create the initial population to be used in the optimization, the non-dimensional variables are randomly selected. A population of 100 elements and a maximum number of 100 iterations are selected. 100 sets of pressure differences randomly selected constitute the first population. The genetic algorithm runs until the convergence is reached, when further changes in population members do not affect the minimal cost obtained. The convergence was reached after about 50-60 generations depending on the thermal load selected. The procedure is shown in Figure 2a. The pressure differences can vary between the values selected in order to obtain, for the most cases simulated, a maximum pressure value lower than the upper pressure limit.

The second optimization is performed using a POD-RBF approach. The POD-RBF model is built using a set of results from the fluid dynamic model. The set of results is called snapshot. In this work each snapshot consists in a set of mass flow rate in the branches where the pumping stations are located and the corresponding pumping cost. Once the model is built, it can be used to simulate different cases respect to the one used to build the model or used as an optimization tool. The procedure is represented in Figure 2b.

The fluid dynamic model is a high time consuming model because it carefully analyzes the system behavior in all the network zones, even when only information in some sections is required (in this case in the booster pumping power branches). The POD-RBF model instead provides an approximate value of the objective function, but the search for the optimum is much faster. These two methods are discussed in detail and compared in the next sections.

3.1 Fluid-dynamic model

A one dimensional model was developed to detail the thermo-fluid dynamic behavior of the main pipeline of the network (i.e. the transport network). The topology of the network has been described using a graph approach [27]. Each pipe is considered as a branch delimited by two nodes, which are identified as the inlet node and outlet node on the basis of a reference direction(velocity is positive when the fluid is flowing in the same direction as the reference direction and negative when flowing in the opposite direction). The main return pipeline network includes 685 branches and 677 nodes, with 9 loops. The fluid-dynamic model

considers the mass conservation equation applied to all the nodes and the momentum conservation equation to all the branches.

The incidence matrix **A**, is used in order to describe the network topology by expressing the connections between nodes and branches. Matrix **A** has as many rows as the number of nodes and as many columns as the number of branches. Its general element A_{ij} is equal to 1 or -1 if the branch j enters or exits the node i and 0 otherwise. Using this matrix the mass balance equation written using matrix form is:

$$\mathbf{A} \cdot \mathbf{G} + \mathbf{G}_{\text{ext}} = 0 \tag{2}$$

where G is the vector that contains the mass flow rates in the branches and $\mathbf{G}_{\text{ext}}$ the vector that contains the mass flow rates exiting the nodes outwards. The terms in $\mathbf{G}_{\text{ext}}$ are different than zero in the case of open networks, i.e. when only a portion of the entire closed circuit is considered.

The steady-state momentum conservation equation in a branch for an incompressible fluid is considered, neglecting the velocity change between input and output sections and including the gravitational term in the static pressure:

$$(p_{\text{in}} - p_{\text{out}}) = \frac{1}{2}\frac{f}{D}L\frac{G^2}{\rho S^2} + \frac{1}{2}\sum_k \beta_k \frac{G^2}{\rho S^2} - t \tag{3}$$

where the first and the second terms on the right-hand side terms are respectively the distributed and the localized pressure losses, while the last term is the pressure rise due to the pumps that may be located in the branch. Equation (3) can be rewritten as:

$$G = Y(p_{\text{in}} - p_{\text{out}}) + Yt \tag{4}$$

where the term Y is the fluid dynamic conductance of the branch, expressed as:

$$Y = R^{-1} = \left[\frac{1}{2}\frac{G}{\rho S^2}\left(\frac{f}{D}L + \sum_k \beta_k\right)\right]^{-1} \tag{5}$$

The friction factor f has been evaluated using an explicit Haaland correlation in order to reduce the computational cost of the simulations.

Momentum equation can rewritten in matrix form. This formulation is obtained using the incidence matrix in order to relate the quantities that are defined at the branches (mass flow rates and pressure variations due to friction and pumping) with pressures at the inlet and outlet nodes:

$$\mathbf{G} = \mathbf{Y} \cdot \mathbf{A}^{\mathrm{T}} \cdot \mathbf{P} + \mathbf{Y} \cdot \mathbf{t} \tag{6}$$

The diagonal matrix **Y** represents the fluid dynamic conductance of branches. Because of the dependence of **Y** on mass flow rate, the obtained system of equation is non-linear. Equation (6) is finally modified by setting proper boundary conditions.

Mass and momentum equations are solved using a SIMPLE (semi implicit method for pressure linked equation) algorithm [28]. This is a guess and correction method: a pressure vector is first guessed and during the iterations it is corrected together with the mass flow rate vector obtained using (6). Further details on the method are available in [29]. In order to solve the system of non-linear equations a fixed point algorithm has been used.

The model includes both the supply and the return pipelines, which are connected in the barycentres. From fluid dynamic viewpoint, barycentres are considered as pipes with their certain friction resistances and the fittings frictions (e.g. T-junctions, curves, etc.). In a general case, the mass flow rates supplied to the barycentres, G_{ut}, differ from their requests, therefore an adjustment is necessary to model the valve controlling the barycentre mass flow rates. Therefore a variable resistance term is added to the fixed term; both resistances are expressed as equivalent lengths which affect the term Y appearing in equation (4).

The variable resistance term is iteratively modified until an acceptable flow distribution is obtained, with all users supplied with the requested mass flow rate. To obtain the mass flow rate required from every user the value of L_{eq} in the n^{th}-iteration is calculated as follows:

$$L_{eq}{}^{n} = L_{eq\_f} + L_{eq\_v}{}^{n-1}\left(\frac{G_{ut}{}^{n-1}}{G_{ut}}\right)^{2} \quad (7)$$

where L_{eq_f} is the fixed resistance and $L_{eq_v}$is the variable resistance. Subscripts n and n-1 refer to the current and previous iterations, respectively. The iterative procedure stops when the relative error between $G^{n-1}$and $G_{ut}$is smaller than a threshold value.

Concerning boundary conditions, the mass flow rate supplied by each plant is fixed on the corresponding node of the supply network. Similarly, the mass flow rate returning at each plant is fixed on the corresponding node on the return network, except for the node corresponding with Moncalieri plant, where the pressure is fixed. The latter boundary condition is required for proper solution of the fluid dynamic problem, as a further condition on the mass flow rate would result in a linearly dependent equation. Pressure is imposed on the Moncalieri plant, since the master pressurizing group is located there.

3.2 Proper Orthogonal Decomposition

Reduced order modeling is an effective way for the development of accurate and computationally inexpensive models. A POD model can be constructed following the method of snapshots, as proposed by Sirovich [30]. A snapshot is a vector **u** of N relevant physical quantities that identify the behaviour of the system for a particular combination of S input parameters, known as the process parameters. The latter are collected in a vector **d**. In this work, pressure rise at the eight booster pumps, the percent thermal load (with respect to the maximum thermal load) and the contribution of each plant to the thermal load are chosen as the process parameters. For a given thermal load and contribution of the various plants, the eight values of pressure rise are the free variables that can be modified in the optimization process. It is worth remarking the fact that pressure rises in the pumps located at the thermal plants are not free variables. These should be adjusted in order to allow circulation of the mass flow rates exiting the various plants.

Table 2 reports the maximum pressure selected for the various booster pumps, obtained after a pre-processing stage, which has been performed in order to limit the number of random combinations of the input that are rejected because of a maximum pressure exceeding the technical limit of 17 bar.

The response **u** of the system to a given set of the free variables is expressed by the mass flow rates at the booster pumps and by the total pumping power.

Different snapshots are obtained by varying the optimization independent variables within a predefined range. In order to avoid obtaining an ill-conditioned model, some precautionary measures have been adopted. First, the input data of the model have been normalized. Furthermore the snapshots have been randomly selected considering a uniform coverage of the input ranges. The complete collection of M snapshots constituted the snapshot matrix **U**. POD aims at approximating an arbitrary snapshot as follows:

$$\mathbf{u}^{\mathrm{a}} = \bar{\Phi} \cdot \bar{\boldsymbol{\alpha}}^{\mathbf{a}} \tag{8}$$

where $\bar{\boldsymbol{\alpha}}^{\mathbf{a}} \in \mathbb{R}^{\mathrm{K}\times 1}$ is a reduced state variable and $\bar{\Phi}$ is an orthogonal matrix. The latter is found solving the following eigenvalue problem [31]:

$$\left(\mathbf{U}^{\mathrm{T}}\mathbf{U}\right) \cdot \boldsymbol{\varphi}_{\mathrm{i}} = \lambda_{\mathrm{i}} \boldsymbol{\varphi}_{\mathrm{i}} \tag{9}$$

Matrix $\bar{\Phi}$ is then built using the eigenvectors $\boldsymbol{\varphi}_{\mathrm{i}}$corresponding to the largest eigenvalues λ_{i}, which are ranked in decreasing order. Namely, $\bar{\Phi} = [\boldsymbol{\varphi}_1, \boldsymbol{\varphi}_2, \dots, \boldsymbol{\varphi}_{\mathrm{K}}]$.

In the present analysis, the POD method has been coupled with radial basis functions (RBF). RBF are typically applied to approximate functions known only in a finite number of points. This interpolation technique involve all known values of functions and it is particularly effective when the distribution of nodes is scattered. Specifically, the reduced state variable $\bar{\boldsymbol{\alpha}}^{a}$ in Eq. (8) has been expressed as a linear combination of radial basis functions of the process parameters p:

$$\bar{\boldsymbol{\alpha}} = \mathbf{B} \cdot \mathbf{g}(d) \tag{10}$$

where **g** contains the radial basis functions and matrix B the coefficients. Here, Euclidean norm was used as RBF:

$$g_i(p) = \|p - p_i\| \quad i = 1, \dots, K \tag{11}$$

Matrix B is found by enforcing that Eq. (10) is exact for each of the snapshots contained in the matrix U [31].

The evaluation of a snapshot corresponding to an arbitrary set of parameter p can be performed using Eq. (12). This is obtained by substituting Eq. (10) in Eq. (8):

$$\mathbf{u} = \bar{\Phi} \cdot \mathbf{B} \cdot \mathbf{g}(p) \tag{12}$$

The entire procedure has been built in Matlab environment. To initialize the POD optimization procedure, a set of random combinations of the free variables has been collected into the initial snapshot matrix **U** and fed as inputs to the full physical model. The corresponding values of mass flow rates in each of the eight pumps and the total pumping costs have been obtained. Snapshots and results are used to create the POD-RBF model, which is the implicit function relating the free variables to the output.

4. Results and discussion

4.1 Full physical model validation

In order to validate the fluid dynamic model in the various operating conditions, a comparison with some measured data of the Turin district heating network was carried out. The pressure differences between two nodes located at the outlet of a pump and at the inlet of the next pump located downstream were evaluated in three different portions of the network where measurements were available for an entire heating season. In Figure 3, the pressure differences are reported as a function of the mass flow rate circulating in the network.

The measured data reported in figure refer to the operating conditions in March, where a large variation takes place. In the figure, the results of the fluid dynamic model are also represented. In the case of the first portion, the model is able to capture the fluid dynamic behavior of the network with high accuracy. In the other sections the dispersion of data is much larger and of the same order as the pressure differences, mainly because these portions are closer to the centre of town, where a large number of sub-networks and buildings are located. In the model, the thermal request profile of the various barycentres was considered similar, i.e. with the same shape parameterized on the basis of the design request. In reality this does not occur. In addition, the model was run considering strict compliance with the control strategy, while in real operation a deviation within an acceptable range is allowed. These are the causes of the large dispersion of data. Anyhow, the average deviation is lower than 0.3 bar, therefore it is possible to state that the fluid dynamic model is able to capture the hydraulic behavior of the network.

4.2 POD model characteristics, validation and performances

Starting from the full physical model, over 15000 simulations were performed, varying the free variables randomly within the predefined ranges. These have been used to create the POD-RBF model.

A test of the POD model was first performed considering new random sets of the free variables, which were not included in the original set. The fluid-dynamics model is used in order to compute the pumping cost, selecting the independent variable randomly, i.e. the pumping pressure differences and the thermal load. The same data are used in order to calculate the output through the POD model. In Figure 4a the POD and Fluid dynamic models' results, in terms of pumping cost, are compared. Results evidently show that the POD based tool in almost all cases is able to reproduce the system behavior.

Mass flow rates obtained from a random set of data using the two models are also computed. For each simulation, the branch containing the booster pumps where the largest mass flow rate is located is analyzed in Figure 4b. The figure shows that the reduced model is able to predict the mass flow rate for all cases with small deviations.

The optimization has been performed for different heat loads. A comparison between the fluid dynamic model and the POD-RBF model is reported in Figure 5. Scenarios have been obtained considering the most typical start-up sequence of the thermal plants. As regards the fluid dynamic model optimization, Figure 5

shows that the larger the thermal load, the larger the optimal pumping cost, except for the scenario corresponding with 40% of the nominal load. The minimum cost for 40% of the nominal load is slightly larger than the minimum cost for 50% of the nominal load. This is due to the fact that when the thermal load is below 40% of the nominal load, only the Moncalieri thermal plant is operating (unless a different order is set, which can occur, for instance, in the case of network maintenance or depending on the production plans, especially related with the electricity production). When the request exceeds 40% of the nominal load, both the Moncalieri and Torino Nord thermal plants are operating. As these plants are located on opposite sides of the network, users in the North areas of the town (closer to Torino Nord plant) are reached by the water flow exiting Torino Nord plant. This allows a reduction in the pressure drops, therefore reducing the pumping cost despite an increase in the total mass flow rate flowing. When the mass flow rate further increases, the pumping cost tends to increase again.

The optimum pumping pressure sets obtained using the POD-RBF model were used as an input in the fluid dynamic model in order to compare the optima. Results show that the POD-RBF model is able to predict the optimal costs as a function of thermal load with average relative errors of about 5%.

A comparison of the computational cost requested to obtain the optimum values with the fluid-dynamic model and the POD-RBF model is reported in Figure 6. Computational costs are evaluated as the summation of the time requested to obtain the minimum cost in all the thermal load conditions that have been analyzed on a single 3.3 GHz CPU. Using the POD-RBF, the total time required for the calculation is reduced by about 95% with respect to that required by the fluid dynamic model.

4.3 POD model for energy cost reduction

4.3.1 Usual start-up sequence of thermal plants

In order to present the potential advantages that can be achieved using an optimized pumping strategy, a comparison between the pumping cost corresponding to the application of a pumping strategy similar to that currently adopted and the optimal strategy is reported in Figure 7. In this analysis, the usual start-up sequence of the thermal plants is considered. It is possible to notice that the use of the optimized control strategy instead of the current one allows the achievement of a significant reduction in the energy consumption for all thermal loads, particularly in the portion between 40% and 90% of the nominal thermal

load. The differences between results obtained with the two optimization strategies (the POD-RBF and the fluid-dynamic model) are quite negligible in comparison with the difference between optimal and current strategy, therefore only the POD-RBF results have been shown, since it is the approach that can be used in real applications.

To better visualize the energy cost reduction with respect to the current pumping strategy, the energy cost reductions in each thermal load is shown in Figure 8. Energy saving is between 8% and 24% and it is particularly large at high thermal load. The use of an optimized pumping strategy allows an annual reduction in primary energy consumption due to pumping of about 4.4 GWh/year (from 25.8 GWh/year in the case of the current strategy to 21.4 GWh/year in the case of the optimized strategy). This represents more than 0.5% reduction in the total primary energy consumption, which is about 842.5 GWh/year (about 768.0 GWh/year associated with heat supplied to the users, about 48.5 GWh/year due to heat losses, and 25.8 GWh/year due to pumping).

These results suggest that application of the POD-RBF optimization approach allows significant improvement in the overall energy performances of large district heating networks.

4.3.2 Different start-up sequence of the thermal plants

The same POD-RBF model can be used in order to optimize the pumping strategy when different combinations of the plants is adopted in thermal production. These scenarios can be necessary in the case one of the plants is not available or if there are specific constraints on the electricity production by the cogeneration plants. When the configuration in heat production changes, also the mass flow rate distribution at the thermal plants change, therefore a different setting of the pumps is necessary, even if the thermal request of the users remains unmodified. The optimization tool should be sufficiently flexible to allow fast optimizations in variable conditions. The POD-RBF model can been used by fixing the total load, by modifying the sequence of thermal plants that are used to cover it and by limiting the maximum DH mass flow rate that is elaborated by each plant (and thus the maximum thermal load supplied by each plant).

Table 3 shows four different scenarios, corresponding with different plant configurations at 60% of the maximum thermal request of the users, are presented. In Figure 9, the corresponding optimal settings of the pumping group obtained using the POD-RBF model are shown.

Results show that the pumping cost is smaller when the two Moncalieri cogeneration plants are not used at 100%. In fact in cases 1 and 2, where just the Moncalieri cogeneration group 1 is switched on the optimal cost is lower than in the cases 3 and 4, where both the cogeneration groups in Moncalieri are used. This is due to the fact that the Moncalieri power plant is located at the south end of the network, therefore when large mass flow rate are supplied by these plants, a large pumping power is necessary. When one of the Moncalieri cogeneration plants is switch off, the power spent to pump the water from the south area to the city centre (R Monc, RP1a, RP1b) is smaller, while the power to pump water from the north to the south is larger (R T.N., R Poli and RP5c). The configuration which minimizes the pumping power corresponds to a more distributed production. In case 1, in fact heat is produced in three plants, one located in the south end (Moncalieri), one in the central area (Politecnico) and one in the north end (Torino nord).

4.3.3 Operation in the case of malfunctioning pumping groups

The POD-RBF model is also been used in order to find the optimal set of pumping pressure when a failure in a pumping station occurs and therefore that piece of equipment cannot be used. In malfunctioning scenarios, minimization of primary energy consumption may become a secondary objective. Nevertheless, the fact that a constrained optimization is performed allows one to obtain the best pumping settings which allow fulfillment of the thermal request of the users, which is instead the main objective in malfunctioning scenarios.

The analysis has been performed for each pumping station. Results are reported in Table 4, considering 60% of the thermal request and the usual configuration for thermal production.

The minimum cost is obtained when no malfunctions occur. Nevertheless in most malfunctioning cases, the optimal costs do not differ significantly with respect to the case without malfunctions, except when a failure occurs in the pump 1b. This is due to the fact that this pump is located in a crucial position for water circulation and its unavailability causes longer paths to reach the users and thus larger friction losses.

Possible iterative interactions between pumping system settings and plant operation can be theoretically examined using the modeling approach proposed in this paper. Such cases are meaningful in the case of possible malfunctions that may affect the hydraulic behavior of the network. In the case there are no pumping strategies that allow proper fulfillment of the thermal request, it is possible to examine scenarios where the production share among the plant is modified in order to help reducing the hydraulic issues.

These results show that POD-RBF model allows one to create a flexible operation tool, which allows optimal management of bot normal and abnormal (malfunctioning) scenarios.

5. Conclusion

The present paper reports an optimization analysis for the minimization of the pumping cost in a large district heating network. The optimization is carried out using two different approaches. The first approach, more conventional, is based on the application of a genetic algorithm to the full physical fluid dynamic model of the network. The second approach utilizes a reduced model, obtained through radial basis function (RBF) and proper orthogonal decomposition (POD) in order to capture the main features of the physical system. This last approach requires much smaller computational time but provides more approximate results due to model reduction. The errors of the POD model in the evaluation of the objective function are quite small.

Fluid dynamic model and the POD-RBF model are used to find the optimal values of pumping cost. Results show that a deviation of about 2% is obtained for both optima. Therefore POD provides a good approximation of the physical behavior of the system. The difference in computational time is very large. This is a crucial feature to allow optimal operation in real networks, as the operating conditions vary significantly depending on the thermal request and the availability of both the thermal plants and the pumping groups. In the case study considered in this paper the calculation of snapshots and the optimization of the POD model requires about 4% of the time requested for the optimization using GA. This difference increases with the number of nodes that are used to represent the network topology, which means that the advantages of using such a technique increases in the case of large networks. In order to show the potential for energy saving in district heating network pumping systems, a comparison between the electricity consumption using the current control strategy and the optimized strategy was carried out. This comparison shows encouraging results which suggest the applicability of fast simulation to the optimal management of the pumping system in district heating networks. The simulation tool shows to be sufficiently flexible to allow one handling both normal operating conditions and malfunctioning conditions.

References

[1] Lund H, Moller B, Mathiesen BV, Dyrelund A. The role of district heating in future renewable energy systems. Energy 2010; 35: 1381–1390.

[2] Roos A, Bohlin F, Hektor B, Hillring B. Woodfuel procurement strategies of district heating plants. Energy 2003; 28: 127–140.

[3] Lindenberger D, Bruckner T, Groscurth HM, Kümmel, R. Optimization of solar district heating systems: seasonal storage, heat pumps, and cogeneration. Energy, 2000; 25: 591-608.

[4] Østergaard PA, Mathiesen BV, Möller B, Lund H. A renewable energy scenario for Aalborg Municipality based on low-temperature geothermal heat, wind power and biomass. Energy 2010; 35: 4892-4901.

[5] Benonysson A, Bohm IB, Ravn HF. Optimization in a District Heating System. Energy Conversion and Management 1995; 36: 297-314.

[6] Pirouti M, Bagdanavicius A, Wu J, Ekanayake J. Optimisation of supply temperature and mass flow rate for a district heating network. Proceedings of ECOS 2012. June 26-29, 2012, Perugia, Italy.

[7] Laajalehto T, Kuosa M, Mäkilä T, Lampinen M, Lahdelma R. Energy efficiency improvements utilising mass flow control and a ring topology in a district heating network. Applied Thermal Engineering 2014; 69: 86-95.

[8] Gustafsson J, Delsing J, Deventer J. Improved district heating substation efficiency with a new control strategy. Applied Energy 2010; 87: 1996‑2004.

[9] Jiang XS, Jing ZX, Li YZ, Wu QH, Tang WH. Modelling and operation optimization of an integrated energy based direct district water-heating system. Energy 2014; 64: 375-388.

[10] Verda V, Baccino G. Primary energy reductions in District Heating Networks through variation of the thermal load profile of the users. Proceedings of ECOS 2014. Turku, Finland, June 15-19.

[11] Jokinen E, Kontu K, Rinne S, Lahdelma R. Demand side management in District Heating buildings to optimize the heat production. Proceedings of ECOS 2014. Turku, Finland, June 15-19.

[12] Tol HI, Svendsen S. Improving the dimensioning of piping networks and network layoutsin low-energy district heating systems connected to low-energy buildings: A case study in Roskilde, Denmark. Energy 2012; 38: 276-290

[13] Koiv TA, Mikola A, Palmiste U. The new dimensioning method of the district heating network. Applied Thermal Engineering 2014; 71(1): 78-82.

[14] Wang H, Yin W, Zhou Z, Lahdelma R. Optimizing the design of a district heating network. Proceedings of ECOS 2015, Pau, France June 30-July 3.

[15] Ancona MA, Melino F, Peretto A. An Optimization Procedure for District Heating Networks. Energy Procedia 2014; 61: 278-281.

[16] Yan A, Zhao J, An Q, Zhao Y, Li H, Huang YJ. Hydraulic performance of a new district heating systems with distributed variable speed pumps. Energy Conversion and Management. 2007; 48: 1536‑1543

[17] Cross H. Analysis of flow in networks of conduits or conductors. Eng Exp Station. 1936; 286: 3‑29;

[18] Stevanovic, VD, Prica S, Maslovaric B, Zivkovic B, Nikodijevic S. Efficient numerical method for district heating system hydraulics. Energy Conversion and Management, 2007; 48(5): 1536-1543.

[19] Ormsbee LE, The History of water distribution Network Analysis: The Computer Age. Proceedings of Water Distribution Systems Analysis Symposium; 2006 August 27-30; Cincinnati, Ohio, USA.

[20] Sciacovelli A, Guelpa E, Verda V, Pumping cost minimization in an existing district heating network. Proceedings of IMECE; 2013 November15-21; San Diego, California, USA.

[21] Lumley JL, Yaglom AM, Tatarski VI. Atmospheric turbulence and radio wave propagation. Journal of Computational Chemistry 1967; 23(13): 1236-1243.

[22] Holmes P, Lumley JL, Berkoz G. The proper orthogonal decomposition in the analysis of turbulent flows. Annu. Rev. Fluid Mech 1993; 25: 539–575

[23] Buljak V. Inverse analyses with model reduction: proper orthogonal decomposition in structural mechanics. Springer Science & Business Media; 2011.

[24] Rosenfeld A, Kak AC. Digital picture processing (Vol. 1). Elsevier; 2014

[25] Tripodi C. Evolution of the Turin District Heating System and the Design of North-West District Network. Energethica. 24-26 May 2012, Turin, Italy (In Italian). http://www.fiper.it/fileadmin/user_upload/news/energethica2012/tripodi.pdf

[26] Golberg DE. Genetic algorithms in search, optimization, and machine learning. Addion wesley; 1989.

[27] Harary F, Graph Theory. Narosa Publishing House, New Delhi; 1995.

[28] Patankar SV. Numerical Heat Transfer and Fluid Flow; 1980.

[29] Sciacovelli A, Verda V, Borchiellini R, Numerical Design of Thermal Systems. Clut, Torino; 2013.

[30] Sirovich L. Turbulence and the dynamics of coherent structures, Parts I, II and III, Q. Appl. Maths XLV, 1987; 561-590.

[31] Ostrowsky Z, Bialecki RA, Kassab AJ.. Advances in application of proper orthogonal decomposition in inverse problems, Proc. 5th Int. Conf. on Inverse Problems in Engineering: Theory and Practice, Cambridge, UK, 11-15th July 2005.

Nomenclature

A	incidence matrix
B	coefficient matrix
c	specific heat, J/(kg K)
C	energy cost, MW
d	input parameters vector
D	pipe diameter, m
f	distributed friction factor
g	radial basis function
G	mass flow rate, kg/s
K	stiffness matrix
L	pipe length, m
M	mass matrix, kg
p	pressure, Pa
P	pressure matrix, Pa
S	pipe section, m^2
t	pumping pressure vector, Pa
T	temperature, °C
u	snapshot
U	snapshot matrix
U	pipe transmittance, W/kg K
Y	fluid dynamic conductance
	Greek symbols
α	coefficient vector

β	localized friction factor
φ	eigenfunction
λ	eigenvalues matrix
ρ	density, kg/m^3
Φ	eigenfunctions matrix
Φ	heat power, MW
	Subscripts and superscripts
ext	external
in	inlet
out	output
ret	return
sup	Supply

507
508

List of Figures

List of Tables

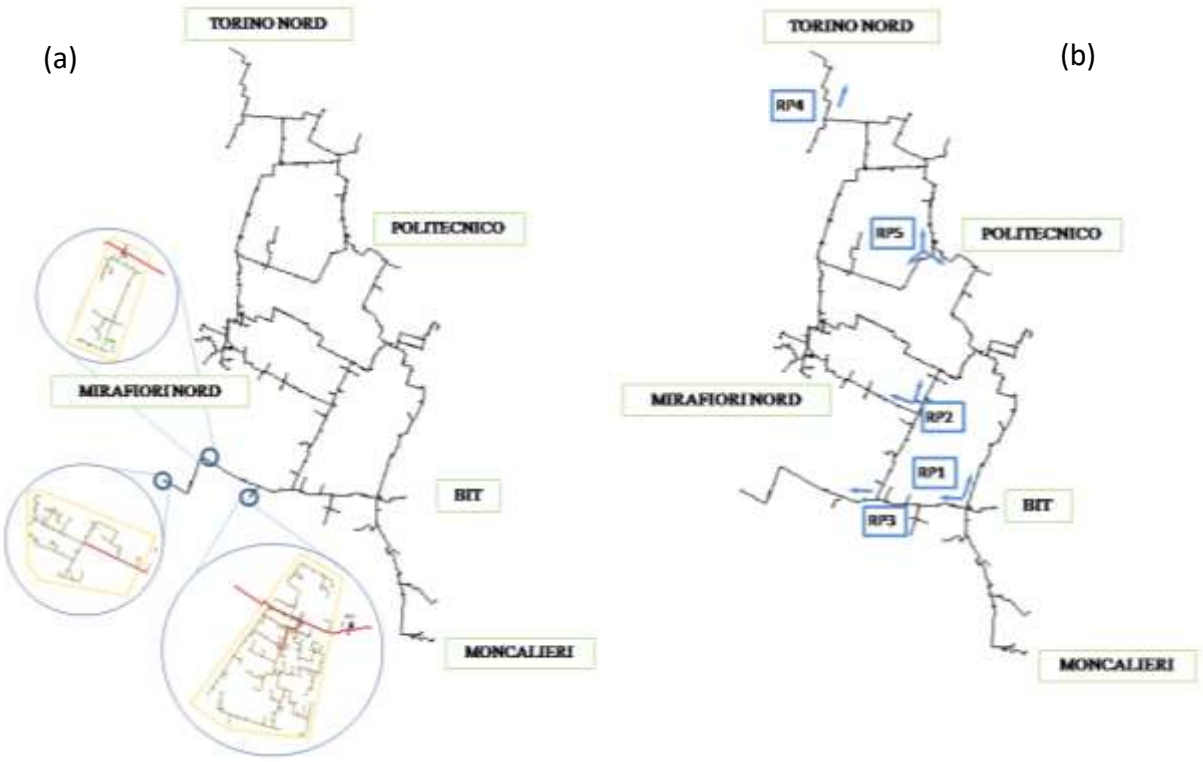

Figure 1: Schematic of Turin District Heating Network (a) In detail 3 barycentres (b) Pumping system

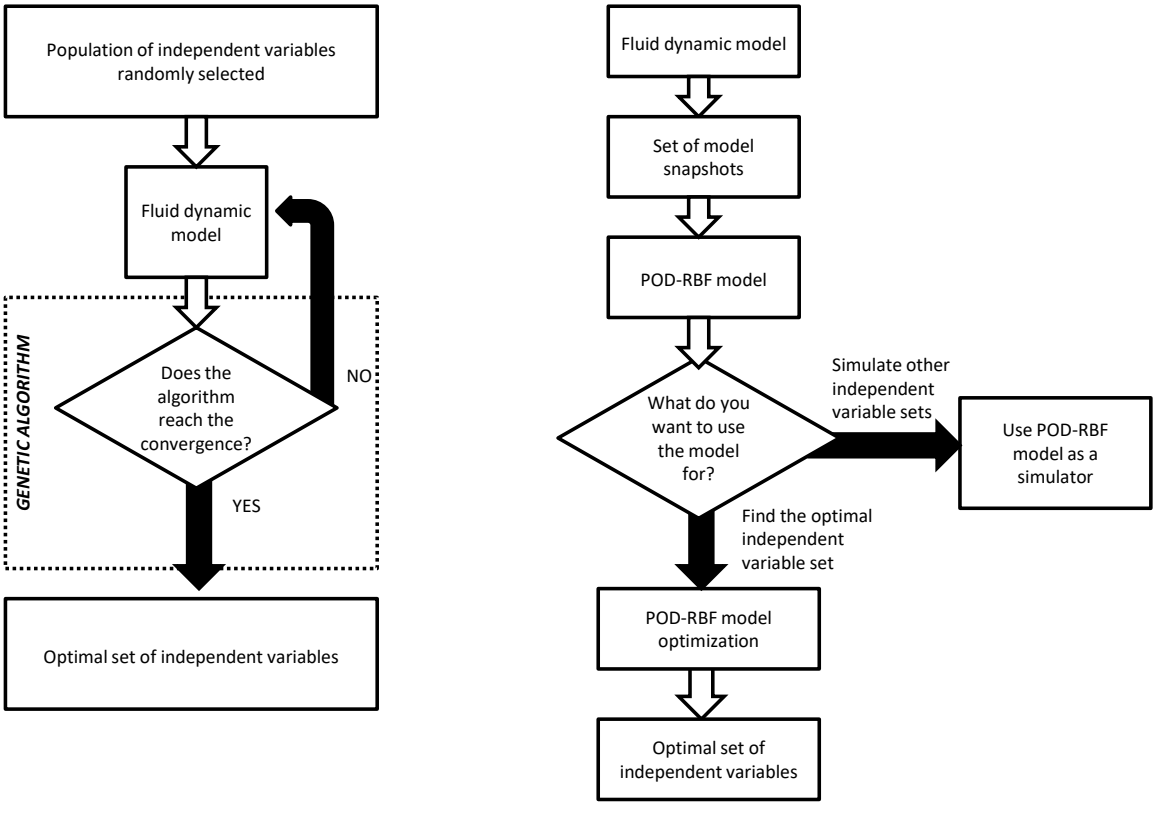

Figure 2: Schematic of the two optimization approaches (a) Fluid dynamic model (b) POD-RBF model

534

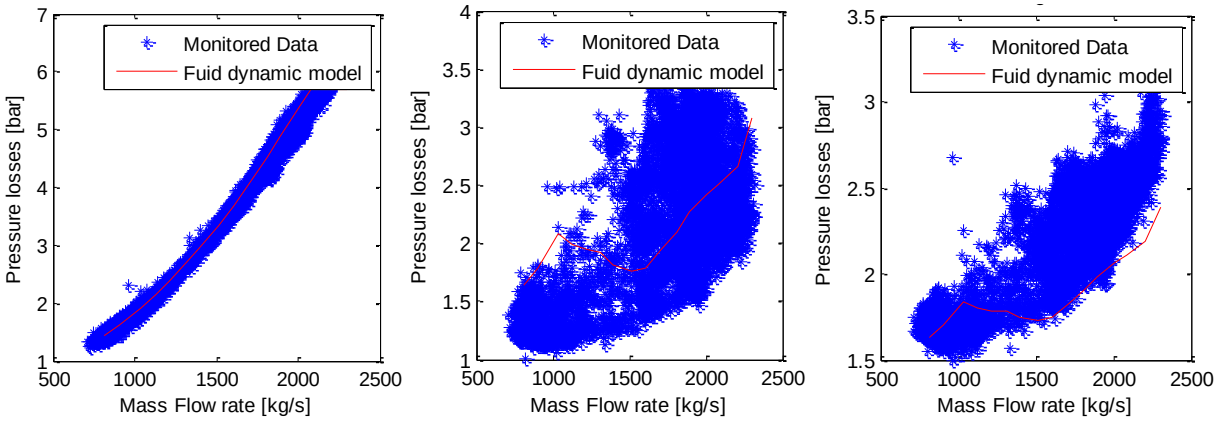

535

536 Figure 3: Test for Fluid dynamic model simulation capability: comparison with measured data

537

538

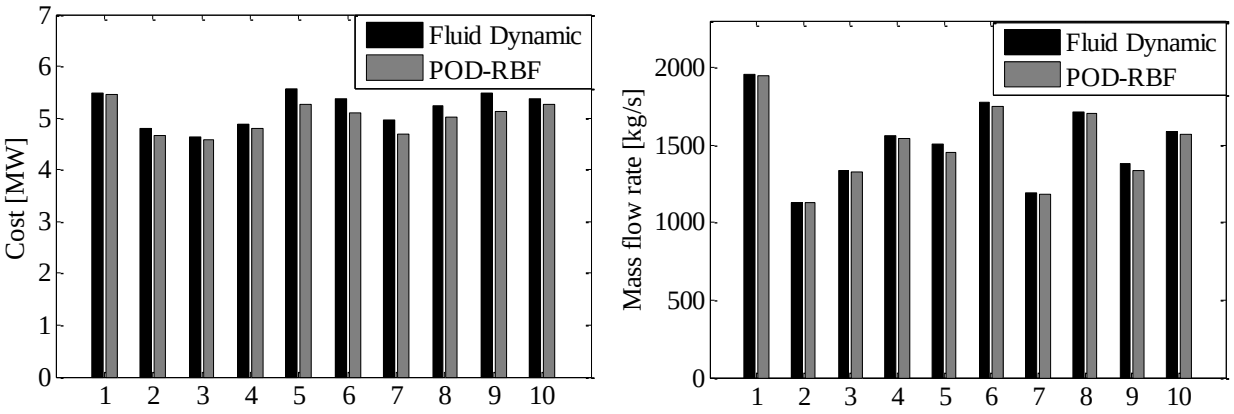

539

540 Figure 4: Test for POD simulation capability with 10 random cases a) pumping costs b) mass flows rate

541

542

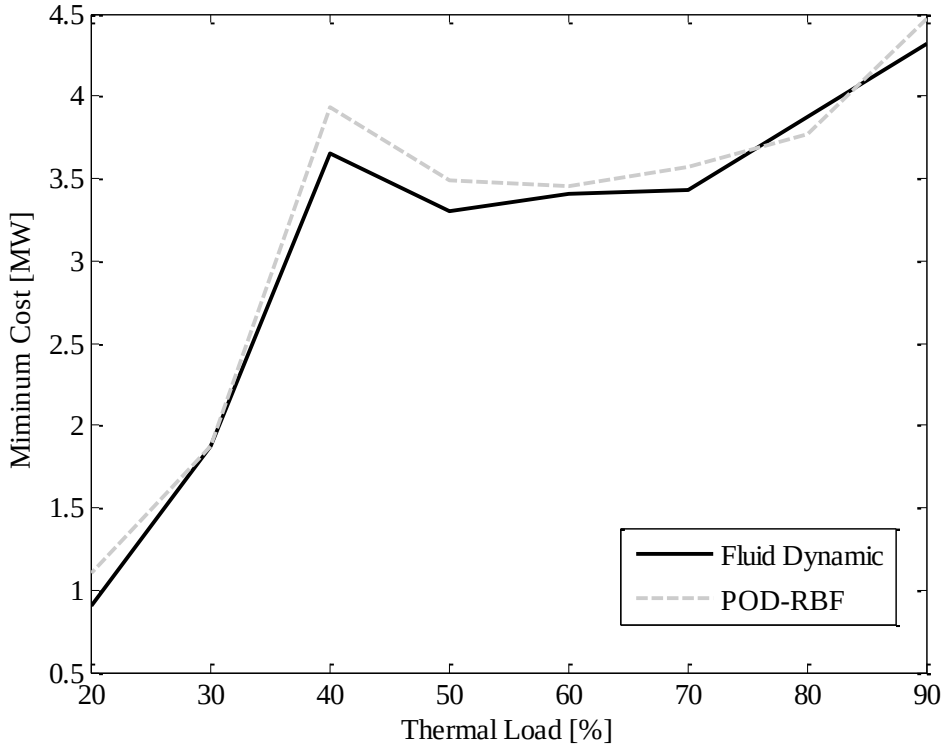

543

544 Figure 5: Best cost comparison

545

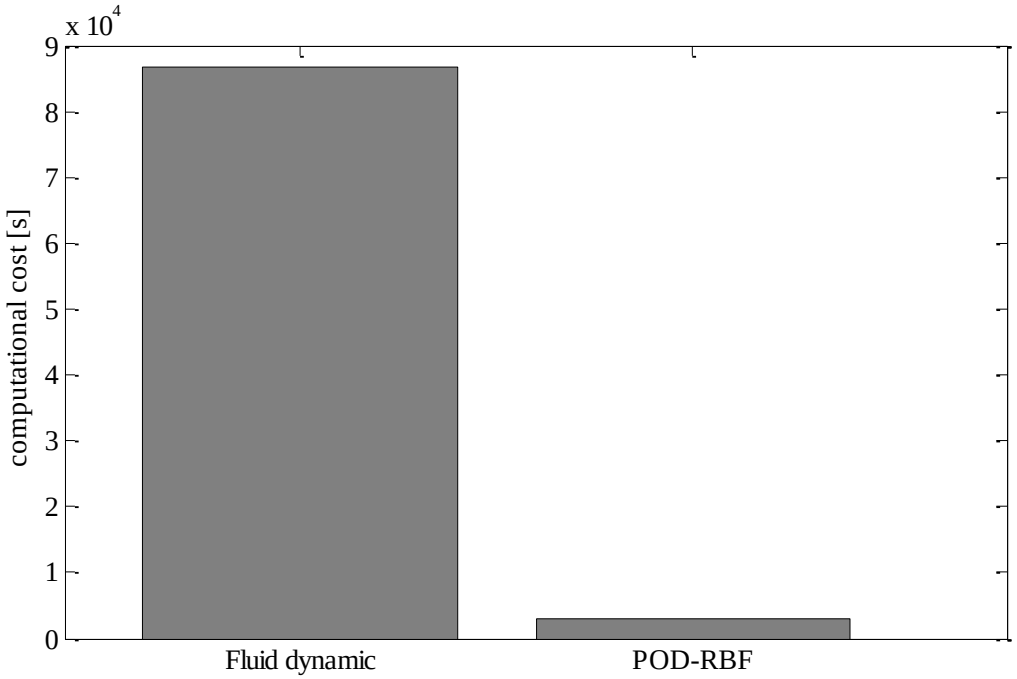

546

547 Figure 6: Computational costs comparison

548

549

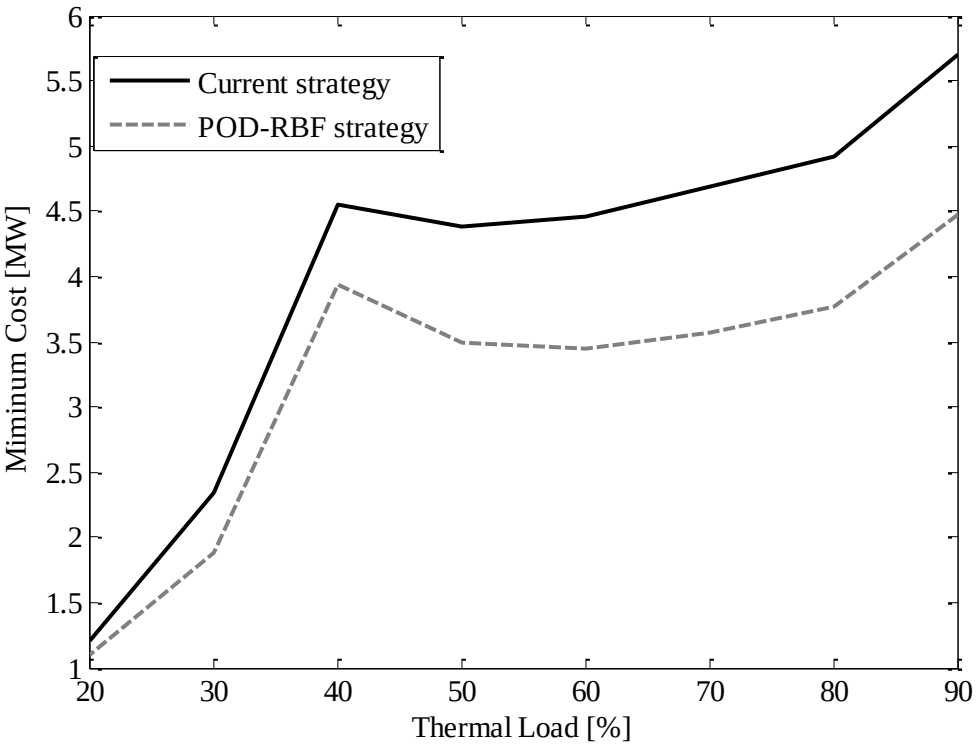

550

551 Figure 7: Energy consumption with current and optimized pumping strategy

552

553

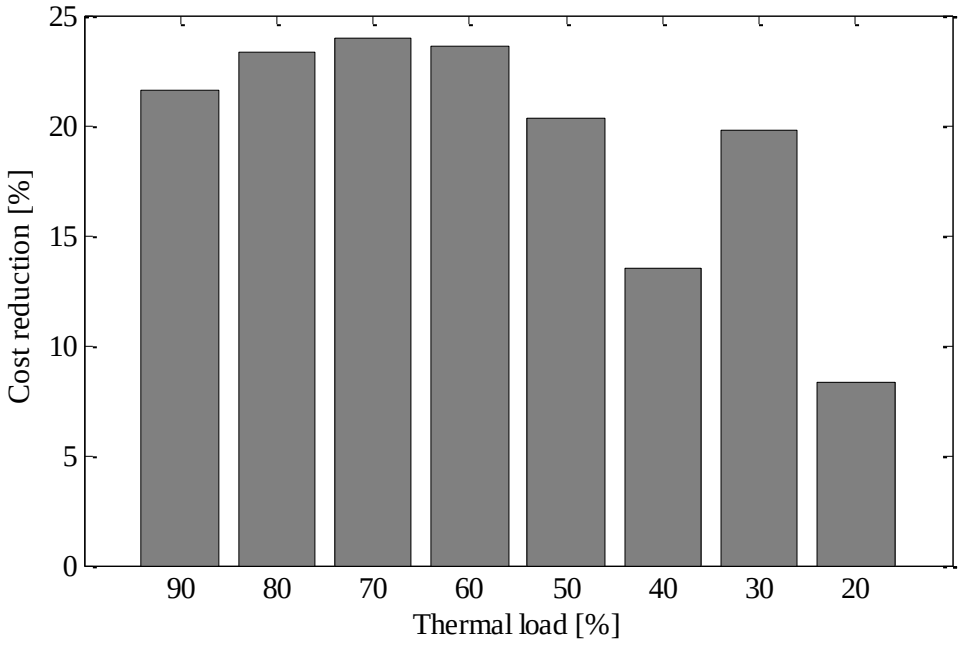

554

555 Figure 8: Energy cost reduction due to use of POD-RBF method instead of current pumps control strategy

556

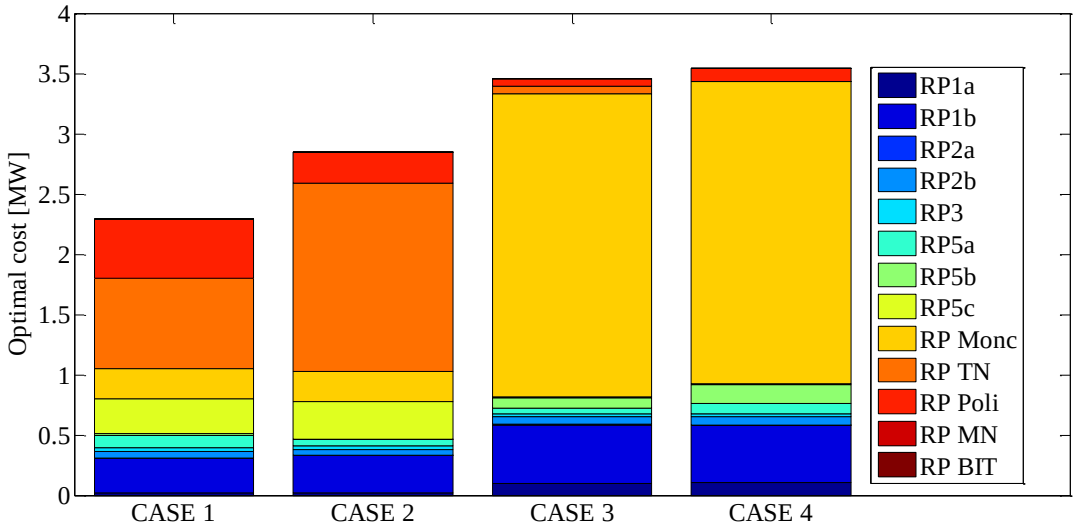

Figure 9: Optimal pumping costs with different plants start up strategy at constant load

Plant	Acronym	Power [MW]	Type
Moncalieri	Monc.	520	Cogeneration (two groups)
		141	Boilers
BIT	BIT	255	Boilers
Mirafiori Nord	M.N.	35	Boilers
Politecnico	Poli.	255	Boilers
		60	Storage
Torino Nord	T.N.	220	Cogeneration
		340	Boilers
		150	Storage

Table 1. Characteristics of the thermal plants

	P_{max} [bar]
RP1a	7
RP1b	7.5
RP2a	6.5
RP2b	7
RP3	6
RP5a	5
RP5b	5
RP5c	5

Table 2. Maximum pressure values for the each booster pumping stations

CASE 1	CASE 2	CASE 3	CASE 4
Monc. Cog. Group 1 T.N. Cog. Politecnico	Monc. Cog. Group 1 T.N. Cog. T.N. Boiler Politecnico	Monc. Cog. Group 1 and 2 T.N. Boiler Politecnico	Monc. Cog. Group 1 and 2 Politecnico

Table 3. Power plants start up strategies considered

	Optimal Cost [W]
No malfunctions	3.57
Malfunction in pump 1a	3.63
Malfunction in pump 1b	4.06
Malfunction in pump 2a	3.58
Malfunction in pump 2b	3.57
Malfunction in pump 3	3.59
Malfunction in pump 5a	3.58
Malfunction in pump 5b	3.60
Malfunction in pump 5c	3.58

Table 4. Minimum costs in case of malfunctions